Check for updates

AGU ADVANCING EARTH AND SPACE SCIENCES

Geophysical Research Letters

RESEARCH LETTER
10.1029/2023GL103952

Freshwater Displacement Effect on the Weddell Gyre Carbon Budget

Benjamin A. Taylor[1,2], **Graeme A. MacGilchrist**[2,3], **Matthew R. Mazloff**[1], **and Lynne D. Talley**[1]

[1]Scripps Institution of Oceanography, University of California San Diego, La Jolla, CA, USA, [2]Program in Atmospheric and Oceanic Sciences, Princeton University, Princeton, NJ, USA, [3]School of Earth and Environmental Science, University of St. Andrews, St. Andrews, UK

Key Points:

- Displacement of seawater by net precipitation and glacial melt is a leading order term in Weddell Gyre dissolved inorganic carbon (DIC) budget
- Evidence is provided by quantifying the DIC mass budget in Biogeochemical Southern Ocean State Estimate (B-SOSE) and regrouping published box inversion results
- In the B-SOSE mean, freshwater displaces 75 Tg DIC/yr, whereas sea ice export drives a 48 Tg DIC/yr lateral import

Supporting Information:

Supporting Information may be found in the online version of this article.

Correspondence to:

B. A. Taylor,
bataylor@ucsd.edu

Citation:

Taylor, B. A., MacGilchrist, G. A., Mazloff, M. R., & Talley, L. D. (2023). Freshwater displacement effect on the Weddell Gyre carbon budget. *Geophysical Research Letters*, *50*, e2023GL103952. https://doi.org/10.1029/2023GL103952

Received 6 APR 2023
Accepted 28 JUL 2023

Author Contributions:

Conceptualization: Benjamin A. Taylor, Graeme A. MacGilchrist, Lynne D. Talley
Data curation: Matthew R. Mazloff
Funding acquisition: Lynne D. Talley
Investigation: Benjamin A. Taylor
Methodology: Benjamin A. Taylor, Graeme A. MacGilchrist
Project Administration: Graeme A. MacGilchrist, Lynne D. Talley
Resources: Graeme A. MacGilchrist, Matthew R. Mazloff
Software: Benjamin A. Taylor, Matthew R. Mazloff

© 2023. The Authors.
This is an open access article under the terms of the Creative Commons Attribution License, which permits use, distribution and reproduction in any medium, provided the original work is properly cited.

Abstract The Weddell Gyre mediates carbon exchange between the abyssal ocean and atmosphere, which is critical to global climate. This region also features large and highly variable freshwater fluxes due to seasonal sea ice, net precipitation, and glacial melt; however, the impact of these freshwater fluxes on the regional carbon cycle has not been fully appreciated. Using a novel budget analysis of dissolved inorganic carbon (DIC) mass in the Biogeochemical Southern Ocean State Estimate, we highlight two freshwater-driven transports. Where freshwater with minimal DIC enters the ocean, it displaces DIC-rich seawater outwards, driving a lateral transport of 75 ± 5 Tg DIC/year. Additionally, sea ice export requires a compensating import of seawater, which carries 48 ± 11 Tg DIC/year into the gyre. Though often overlooked, these freshwater displacement effects are of leading order in the Weddell Gyre carbon budget in the state estimate and in regrouped box-inversion estimates, with implications for evaluating basin-scale carbon transport.

Plain Language Summary The ocean surrounding Antarctica plays a key role in the global carbon cycle because it is one of the few places where carbon-enriched abyssal waters can exchange with the atmosphere. Here we focus on the Weddell Gyre that covers the Atlantic sector poleward of 60°S; this region features enormous exchanges of freshwater through the surface, via sea ice that covers the region each winter, frequent precipitation, and land ice melting into the ocean. Using a model that assimilates available observations, we explore how this freshwater affects the region's ability to transport carbon between the atmosphere and deep ocean. Whereas previous studies have focused on how springtime sea ice melt dilutes surface ocean carbon concentrations, we emphasize that throughout the year, adding water with minimal carbon (from rain, snow, or land ice) to the ocean displaces carbon-rich seawater. Second, sea ice melt and formation alone do not displace seawater, but when sea ice flows out of the region, carbon-rich seawater responds by flowing in the opposite direction. These freshwater displacement effects are leading order terms of the regional carbon budget in our model analysis and in our reconsideration of past observational estimates.

1. Introduction

The Weddell Gyre has a key role in the global oceanic carbon cycle, particularly in mediating exchange between the abyssal ocean and the atmosphere (Sarmiento & Toggweiler, 1984; Sigman et al., 2010; Stephens & Keeling, 2000). As part of the Antarctic sea-ice zone, it brings the densest waters of the global ocean into contact with the atmosphere, though CO_2 equilibration often remains incomplete (Hoppema et al., 2001; Murnane et al., 1999), and transports them into the "lower cell" of the global overturning circulation (Jullion et al., 2014) where they are sequestered for millennia. The net regional air-sea fluxes of climate-relevant constituents such as heat and dissolved inorganic carbon (DIC) are balanced primarily by net oceanic transport between the gyre and the Antarctic Circumpolar Current (ACC) to the north. Thus, the processes that control the long-term net carbon transport into the Weddell Gyre are of broad scientific interest (Vernet et al., 2019). This carbon transport has been associated with the southward upwelling of DIC-rich deep waters via the overturning circulation (Brown et al., 2015; Iudicone et al., 2011), though detailed regional study has noted that the net outward (i.e., northward) DIC transport must be driven by processes other than the overturning (MacGilchrist et al., 2019). The overturning circulation is shaped by freshwater fluxes in the sea-ice covered Southern Ocean (Pellichero et al., 2018): Brine rejection due to sea ice formation and super-cooled melt water from ice shelves and ocean-terminating glaciers are key components of dense shelf overflows (Nicholls et al., 2009), whereas sea ice melt, together with net precipitation, lightens upper ocean waters as they are transported northward in the surface Ekman layer (Abernathey et al., 2016). However, freshwater fluxes have another, more basic, effect on ocean circulation: an

Supervision: Graeme A. MacGilchrist, Lynne D. Talley
Validation: Matthew R. Mazloff
Visualization: Benjamin A. Taylor
Writing – original draft: Benjamin A. Taylor
Writing – review & editing: Benjamin A. Taylor, Graeme A. MacGilchrist, Matthew R. Mazloff, Lynne D. Talley

addition of freshwater at the surface displaces the water below, causing a divergent mass transport (Huang & Schmitt, 1993) that may carry significant quantities of carbon (Robbins, 2001). The impact of this relatively weak circulation on net carbon transport into and out of the Weddell Gyre, or any region of the Southern Ocean, has not been explored.

Several balances comparing the processes that affect Weddell Gyre surface ocean DIC concentration (Brown et al., 2015; Hoppema et al., 1999; Rosso et al., 2017) agree that freshwater fluxes play a key role by diluting DIC concentration, especially during the spring sea ice melt. Previous analysis of the Biogeochemical Southern Ocean State Estimate (B-SOSE) (Rosso et al., 2017) suggests that freshwater dilution is a leading source of upper ocean DIC variability in the sea-ice zone; further north where stronger outgassing is observed (Gray et al., 2018), DIC advection including Ekman-driven upwelling is more dominant. In addition to dilution, freshwater input also increases stratification, favoring greater net biological export, and slightly encourages air-sea carbon uptake (though the effect of DIC dilution on pCO_2 is muted by the concurrent decrease in alkalinity). A change in DIC concentration via dilution, however, does not imply a change in DIC mass (the total number of moles of DIC) (see Figures 1a and 1b, center). For instance, in the limit of sea-ice as pure freshwater, sea ice melt does not change the total mass of DIC in a region of the ocean; it simply redistributes the same DIC mass into a slightly larger volume of water. Indeed, published budgets of total DIC mass in the Weddell Gyre (Brown et al., 2015; MacGilchrist et al., 2019) do not emphasize the role of freshwater fluxes, in marked contrast to the upper ocean concentration balances.

In the traditional box model framework for regional budgets, the time-mean transport of a conserved tracer (such as heat or DIC mass) across the lateral boundary is primarily balanced by the mean air-sea flux and the change in tracer content within the region (Hall & Bryden, 1982; Jullion et al., 2014; Roemmich & Wunsch, 1985). This framework has proven practical value for DIC, because the transport term can be directly estimated from oceanographic sections along the boundary of the region, allowing an independent estimate of the mean air-sea flux (Álvarez et al., 2003; Brewer et al., 1989; Broecker & Peng, 1992; Holfort et al., 1998; Sarmiento et al., 1995). This is particularly helpful in the presence of sea-ice, which hinders net air-sea gas exchange (though to what extent remains poorly constrained (Delille et al., 2014)). The box model framework is also helpful in understanding the mean air-sea exchange: by integrating through the many compensating transports of carbon in the upper ocean, it highlights processes with a net effect (MacGilchrist et al., 2019).

Here, we examine the Weddell Gyre DIC mass budget to better understand the role of freshwater fluxes in the horizontal DIC transports that balance air-sea CO_2 uptake. Namely, we find that freshwater processes significantly impact DIC mass via displacing seawater, driving net volume flow and carbon transport at the lateral boundary. We call this the freshwater displacement effect (Figures 1a and 1b). While this is a well-known aspect of salt budgets (Tréguier et al., 2014), it has received relatively little attention as a significant term in the carbon budget, with the important exception of Robbins (2001). However, a back-of-the-envelope calculation suggests a magnitude on the order of air-sea gas exchange in the Weddell Gyre: a net displacement of ocean water of 50 mSv due to P-E+R (Jullion et al., 2014) and a mean ocean concentration of 2.24 mmol DIC/kg would yield a transport of 45 Tg DIC/yr, comparable to the estimates of 30–58 Tg C/yr of uptake from the atmosphere (Brown et al., 2015). The importance of this term stems from the fact that seawater leaving the region has vastly greater concentrations of carbon than the freshwater entering the ocean.

We explore this freshwater displacement effect through a DIC mass budget derived from B-SOSE, which assimilates year-round physical and biogeochemical observations of the Southern Ocean into a dynamically consistent model with active mesoscale eddies (Verdy & Mazloff, 2017). Previously, B-SOSE was run with freshwater input represented by virtual salt fluxes, so displacement effects were absent; here, we use a realistic freshwater scheme that conserves DIC mass. We consider the displacement effect of various freshwater fluxes on the DIC mass inventory (i.e., total moles of DIC) within our region of study, which is chosen to facilitate comparison with estimates derived from hydrography (Brown et al., 2015; Jullion et al., 2014). We note that addition of freshwater (via precipitation or glacial runoff) and sea ice export both drive a net transport of seawater and thus DIC through the lateral boundary of the region (Figure 1). We show that in B-SOSE, the associated transports are significant in both the seasonal cycle and the annual average; since B-SOSE contains significant known biases in this region (Figure S1 in Supporting Information S1), we separately evaluate these transports using existing box-inverse estimates from Brown et al. (2015). Finally, we estimate the significance of the freshwater displacement effect for Southern Ocean meridional carbon transport.

19448007, 2023, 18, Downloaded from https://agupubs.onlinelibrary.wiley.com/doi/10.1029/2023GL103952 by University Of California, Wiley Online Library on [20/02/2024]. See the Terms and Conditions (https://onlinelibrary.wiley.com/terms-and-conditions) on Wiley Online Library for rules of use; OA articles are governed by the applicable Creative Commons License

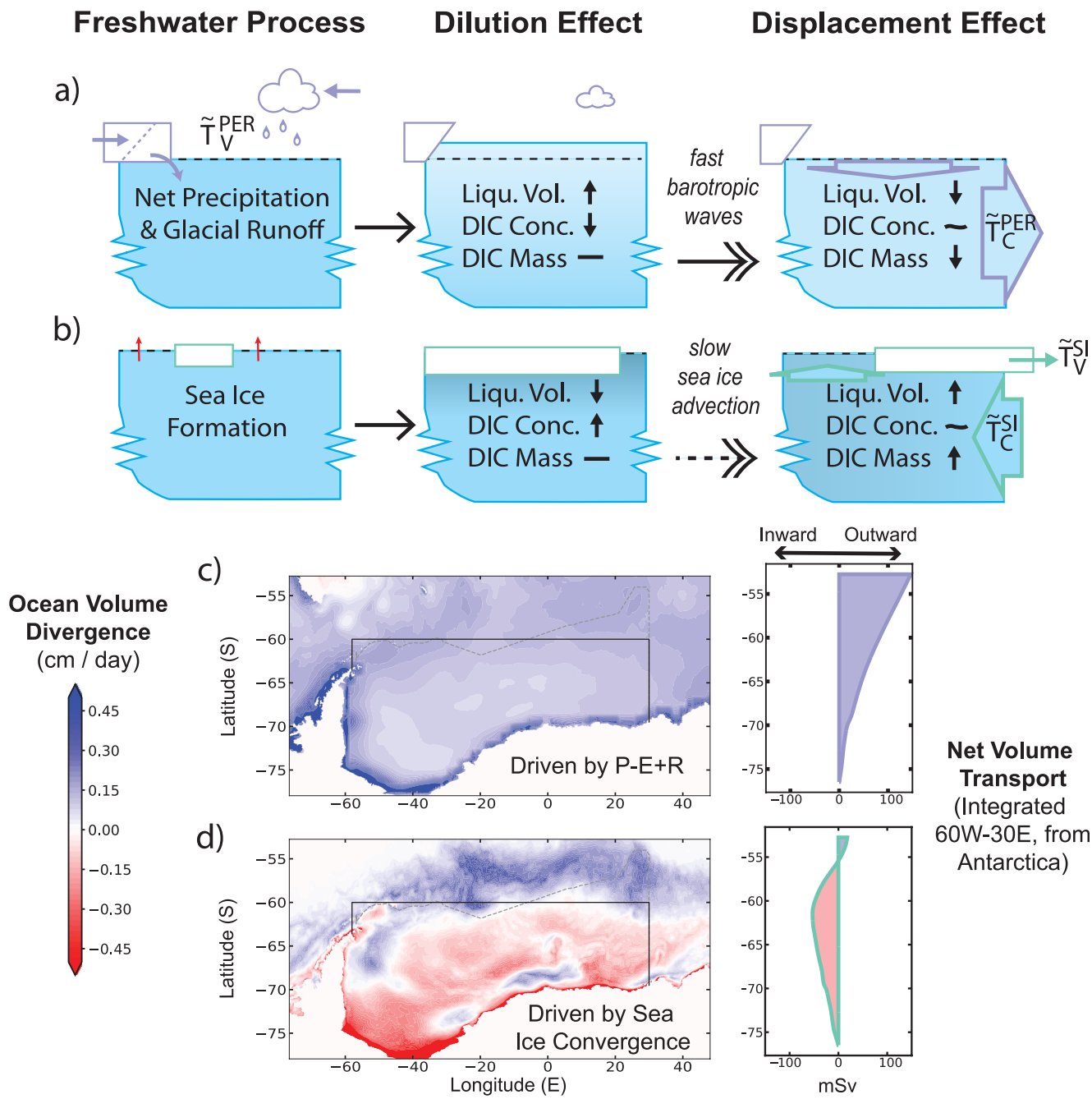

Figure 1. Overview of Freshwater Displacement Effect on the Weddell Gyre. Panels (a)–(b) show the Weddell Gyre box response to freshwater processes, including dilution effects on dissolved inorganic carbon (DIC) concentration and displacement effect on circulation and DIC mass. Shading reflects DIC concentration (darker blue = more DIC), and the dashed black line is mean dynamic sea level (the vertical scale is vastly exaggerated near the surface). (a) Net precipitation and glacial melt dilute seawater and temporarily raise sea level, rapidly triggering an outflow $\tilde{T}_C^{PER}$ via barotropic waves. (b) Sea ice formation concentrates sea water via brine rejection, but (assuming sea ice carries minimal DIC) sea ice only affects DIC mass via transport across the region's boundary. (c)–(d) Map the components of B-SOSE 2013–2021 average ocean volume divergence into the Weddell region in cm/day on the left, then show the quantity integrated (south of the given latitude and between 60°W and 30°E) into a total outward volume transport. The black lines outline our "Weddell Gyre" box, while gray dashed lines show the track of the ANDREX cruises used for the box inverse estimate. (c) Net Precipitation - Evaporation - (glacial) Runoff (P-E+R) is plotted. Precipitation and runoff invoke ocean volume divergence, whereas evaporation drives convergence. (d) Convergence of sea ice volume is plotted; convergence of sea ice volume implies ocean volume divergence.

19448007, 2023, 18, Downloaded from https://agupubs.onlinelibrary.wiley.com/doi/10.1029/2023GL103952 by University Of California, Wiley Online Library on [20/02/2024]. See the Terms and Conditions (https://onlinelibrary.wiley.com/terms-and-conditions) on Wiley Online Library for rules of use; OA articles are governed by the applicable Creative Commons License

19448007, 2023, 18, Downloaded from https://agupubs.onlinelibrary.wiley.com/doi/10.1029/2023GL103952 by University Of California, Wiley Online Library on [20/02/2024]. See the Terms and Conditions (https://onlinelibrary.wiley.com/terms-and-conditions) on Wiley Online Library for rules of use; OA articles are governed by the applicable Creative Commons License

2. Methods

2.1. Model

This study employs output from B-SOSE (Verdy & Mazloff, 2017), iteration 139, which is a 1/6° state estimate of the 2013–2021 period. This product assimilates numerous physical and biogeochemical data sources, with particular attention to the novel BGC-Argo floats (Talley et al., 2019) making year-round measurements in the ice-covered Southern Ocean during this time period. B-SOSE employs the adjoint method of data assimilation to produce a physically consistent solution, allowing the production of closed budgets for tracers of interest (Rosso et al., 2017). Sea ice in B-SOSE includes realistic heat fluxes and material properties, but chemically it is represented as pure water; similarly, land ice and freshwater input have no biogeochemical tracers in this iteration.

To clarify the effect of freshwater fluxes on DIC inventory, we run B-SOSE with a real freshwater flux and nonlinear free surface (Campin et al., 2004). This represents a departure from previous B-SOSE runs including Iteration 122, which employed a virtual tracer flux (Rosso et al., 2017). This previous approach represented only the dilution effect of freshwater input/loss, resulting in the dilution of tracer concentration via unphysical removal/addition of tracer to the ocean surface layer, which violates the conservation of tracer mass. The virtual tracer flux is often referred to as a virtual salt flux; in biogeochemical ocean models run with this configuration, all dissolved seawater constituents including DIC experience the unphysical "virtual" flux. In the new configuration, this concentration change is more accurately represented by the addition of water, which modifies the model's free surface to produce a nonzero velocity potential (i.e., divergent) flow that drives the displacement effect and conserves tracer mass (Griffies et al., 2001).

2.2. DIC Inventory Budget

Here we describe the procedure for assembling a DIC mass budget from the output of B-SOSE that explicitly represents the freshwater displacement effects; the full mathematical derivation is shown in Text S1 in Supporting Information S1. Northward (and eastward) transports are defined as positive; thus a positive transport removes DIC from our region of interest. For each model grid cell, we save the components of the local DIC mass budget (all with units g C/s): the time-tendency of carbon mass ($TEND$) is balanced by advection (ADV), diffusion (DIF), biological sources and sinks (BIO), and air-sea gas exchange $\left(F_{CO_2}\right)$

$$TEND = ADV + DIF + BIO + F_{CO_2}. \tag{1}$$

Note that, in an important deviation from previous B-SOSE analysis in Rosso et al. (2017), each term is a change in DIC mass, not concentration; thus there is no term in this budget corresponding to "dilution." We then sum the cells within the full-depth Weddell Gyre, here defined as the region of ocean within the black boxes in Figures 1c and 1d. The summed advection (ADV) is equal to the carbon transport inwards across the lateral boundary of our domain; we label the outward transport T_C (units g C/s), so that $T_C = -\sum ADV$.

While freshwater exchange across the ocean surface does not carry carbon in B-SOSE, it does invoke a volume transport that drives a component of T_C. To evaluate this, we decompose T_C into a component associated with the divergent volume transport (labeled $\tilde{T}_C$) and a remainder with no net volume transport (labeled $\hat{T}_C$):

$$T_C = \tilde{T}_C + \hat{T}_C = \tilde{T}_V \overline{C} + \hat{T}_C. \tag{2}$$

The "non-divergent" transport $\hat{T}_C$ reflects the differences in DIC concentration between outflowing and inflowing seawater, including the effects of the overturning circulation and any horizontal circulation. On the other hand, the divergent carbon transport $\left(\tilde{T}_C\right)$ is driven by the total volume transport out of the domain ($\tilde{T}_V$, units m^3/s), since the section-mean carbon concentration $\left(\overline{C}\right)$ varies little in time. We have

$$\tilde{T}_V = \tilde{T}_V^{PER} - \tilde{T}_V^{SI} + \tilde{T}_V^{\partial t}, \tag{3}$$

where $\tilde{T}_V^{PER}$ is total meteoric (net precipitation and land ice) input which drives volume northward out of the domain; $\tilde{T}_V^{SI}$ is positive sea ice export (which includes a factor for sea-ice/seawater density difference) and causes volume to enter the domain; and $\tilde{T}_V^{\partial t}$ is the area-average transient sea level change, which has no net effect but can be large at short timescales (see Text S1, Figure S2 in Supporting Information S1 for details). Substituting our expression for $\tilde{T}_V$ into Equation 2, we can write the total transport as

$$T_C = \overline{C}\left(\tilde{T}_V^{\partial t} + \tilde{T}_V^{PER} - \tilde{T}_V^{SI}\right) + \hat{T}_C$$
$$= \tilde{T}_C^{\partial t} + \tilde{T}_C^{PER} + \tilde{T}_C^{SI} + \hat{T}_C. \quad (4)$$

Here, we have introduced carbon transports $\tilde{T}_C^{PER} = \tilde{T}_V^{PER}\overline{C}$ and $\tilde{T}_C^{SI} = -\tilde{T}_V^{SI}\overline{C}$ (units g C/s), which are the two freshwater displacement effects. $\tilde{T}_C^{PER}$ is the DIC transport in response to Precipitation - Evaporation + Runoff (PER), which is positive for a positive net precipitation; $\tilde{T}_C^{SI}$ is the inward (negative) transport of DIC in response to sea ice export (SI). We have also introduced $\tilde{T}_C^{\partial t}$, which is the effect of transient sea level changes on carbon transport. Substituting our decomposition of $T_C = -\sum ADV$ into the regionally summed carbon budget (Equation 1) provides our final carbon inventory budget:

$$\sum TEND - \tilde{T}_C^{\partial t} = -\tilde{T}_C^{PER} - \tilde{T}_C^{SI} - \hat{T}_C + \sum(BIO + F_{CO2}) \quad (5)$$

(where $\tilde{T}$ describes terms associated with net volume transport, and $\hat{T}_C$ is the remaining non-divergent carbon transport). In writing this inventory budget, we evaluate the transient sea level term $\left(\tilde{T}_C^{\partial t}\right)$ together with the tendency of DIC mass, so that the noisy oscillations in volume due to sea level change are removed from the DIC "inventory." We have also discarded the diffusion term (DIF) since it is negligibly small in the full-depth sum.

3. Results

While dilution of seawater affects the DIC concentration, only displacement of seawater changes the regional total DIC mass (Figures 1a and 1b). Sea ice net melt is the most prominent component of the Weddell freshwater fluxes (Figures S2b and S2c in Supporting Information S1), and plays a dominant role in shaping the DIC concentrations in the surface ocean via dilution (Rosso et al., 2017). However, sea ice melt and formation do not cause a circulation response and therefore do not transport DIC, as shown schematically in Figure 1b. Net P-E+R (Figure 1a) and sea ice export (Figure 1b) do displace seawater, which transports carbon; their spatial distributions in the Weddell Gyre are shown in Figures 1c and 1d. Precipitation exceeds evaporation throughout the region, whereas glacial runoff is concentrated at the coasts. Sea ice divergence (negative convergence) is also strong at the coasts, where katabatic winds drive sea ice formation (Thompson et al., 2020), while sea ice converges (and melts) at the northern rim of the gyre where it contacts warm ACC waters (Abernathey et al., 2016).

The evaluation of Equation 5 in B-SOSE over our 2013–2021 run is shown in Figures 2a–2d. Whereas previous carbon concentration budgets have been dominated by the sea ice melt and formation, this DIC mass budget displays five processes of similar magnitude—including the two displacement effects. Year-round displacement of high carbon water by net precipitation and runoff $\left(\tilde{T}_C^{PER}\right)$ transports 75 ± 5 Tg DIC/year out of the gyre; this is partially offset by $\tilde{T}_C^{SI}$ adding 48 ± 11 Tg DIC/year into the region (Figure 2b). During the ice-covered "winter" (Figure 2c), $\tilde{T}_C^{SI}$ is the leading process transporting DIC into the gyre; in late winter, the mass export of sea ice exceeds the mass gain of net P-E+R, so that the usual outward $\tilde{T}_V$ reverses direction and $\tilde{T}_C$ transports DIC into the gyre. In this inventory budget perspective, $\tilde{T}_C^{PER}$ is a crucial component of the carbon system throughout the year, and $\tilde{T}_C^{SI}$ and $\tilde{T}_C^{PER}$ dominate the wintertime balance.

Our budget also shows the important role of several more familiar processes, particularly in the better-observed ice-free season (Figure 2b). Non-divergent carbon transport $\hat{T}_C$ largely reflects the overturning circulation, which steadily imports deep water with more DIC than the outflowing surface or abyssal waters. We note a seasonal cycle in $\hat{T}_C$: the 72 ± 21 Tg DIC/yr import in the ice-free summer is significantly higher than the wintertime 38 ± 18 Tg DIC/yr, because the outflowing near-surface DIC concentrations are reduced by dilution, biological consumption, and subdued mixing during summer (Brown et al., 2015). Phytoplankton consume DIC during the spring bloom and organic matter gradually remineralizes over the winter season, the two largely compensating each other in the annual average. However, a consistent small loss of DIC (7 Tg DIC/yr) can be partly attributed to the lateral transport of dissolved organic carbon out of the region in the surface Ekman layer (Figure S3 in Supporting Information S1). There is an air-sea carbon uptake for nearly the entire open-water period; the resulting small annual sink of 33 ± 5 Tg DIC/yr (Figure 2d) compares well with observational estimates (e.g., 33 ± 21 Tg/yr DIC, Brown et al. (2015), Section 5.3). This air-sea uptake correlates significantly ($p < 0.02$) with the lateral DIC transport, and with $\tilde{T}_C^{SI}$ in particular, on interannual timescales (see Figure S4 in Supporting Information S1). Finally, the increase in DIC inventory in B-SOSE largely reflects anthropogenic carbon storage, but also includes model drift; see Text S2, Figure S5 in Supporting Information S1.

19448007, 2023, 18, Downloaded from https://agupubs.onlinelibrary.wiley.com/doi/10.1029/2023GL103952 by University Of California, Wiley Online Library on [20/02/2024]. See the Terms and Conditions (https://onlinelibrary.wiley.com/terms-and-conditions) on Wiley Online Library for rules of use; OA articles are governed by the applicable Creative Commons License

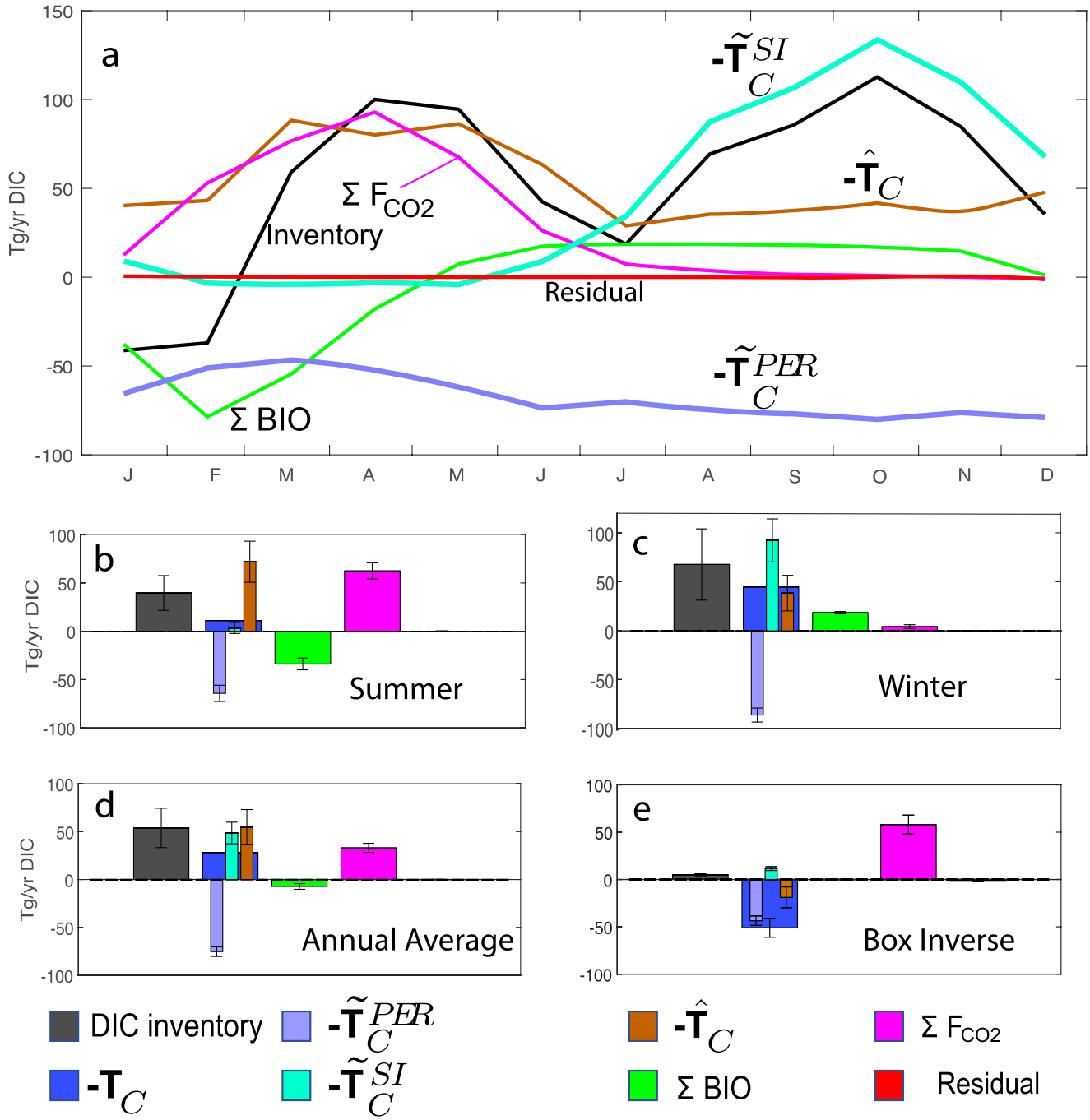

Figure 2. Weddell Gyre dissolved inorganic carbon (DIC) inventory budget in B-SOSE. Positive terms increase DIC in the Weddell Gyre, so our northward transports appear with negative signs. (a) Seasonality of each term in Equation 5, over the period 2013–2021. (b) "Summer" (mid-December through mid-June) mean of terms in (a), as well as negative total advection $\left(T_C = \hat{T}_C + \tilde{T}_C^{PER} + \tilde{T}_C^{SI}\right)$. Uncertainties show the interannual variability of the quantity within the model period. (c) "Winter" (mid-June through mid-December) mean of terms in (b). (d) Annual average of terms in (b). (e) Inverse-derived DIC budget from Brown et al. (2015), with advection term decomposed as in (b).

Our DIC inventory perspective facilitates comparison with a box inverse model-derived full-depth carbon budget of the Weddell Gyre from the ANDREX experiment (Brown et al., 2015; Jullion et al., 2014; MacGilchrist et al., 2019), especially with regard to the freshwater displacement effects. ANDREX in situ observations were collected over two austral summers (2008–2009, 2009–2010); from these and the 2008 I06S line, Jullion et al. (2014) derived a box inverse model solution for the Weddell Gyre. Brown et al. (2015) applied the derived

19448007, 2023, 18, Downloaded from https://agupubs.onlinelibrary.wiley.com/doi/10.1029/2023GL103952 by University Of California, Wiley Online Library on [20/02/2024]. See the Terms and Conditions (https://onlinelibrary.wiley.com/terms-and-conditions) on Wiley Online Library for rules of use; OA articles are governed by the applicable Creative Commons License

19448007, 2023, 18, Downloaded from https://agupubs.onlinelibrary.wiley.com/doi/10.1029/2023GL103952 by University Of California, Wiley Online Library on [20/02/2024]. See the Terms and Conditions (https://onlinelibrary.wiley.com/terms-and-conditions) on Wiley Online Library for rules of use; OA articles are governed by the applicable Creative Commons License

velocities to the measured DIC concentrations to calculate the total DIC transport and thereby estimate air-sea uptake of carbon as the residual. Using freshwater and sea ice transports from Jullion et al. (2014), we decompose the ANDREX total DIC transport into our three terms: P-E+R, sea ice, and non-divergent advection (Figure 2e), as opposed to the watermass decomposition of the previous publications. Jullion et al. (2014) found 50 ± 5 mSv of P-E+R, which was balanced by 15 ± 2 mSv of sea ice volume export and a $\tilde{T}_V = 36 \pm 190$ mSv volume export (the large uncertainty is associated with transient barotropic flow, i.e., $\tilde{T}_V^{\partial t}$). Using a DIC concentration representative of the section-mean (2.3 mol/m^3) and sea ice/seawater density ratio of 0.88, we estimate a $\tilde{T}_C^{PER}$ of 44 ± 5 Tg DIC/yr and a $\tilde{T}_C^{SI}$ of −12 ± 2 Tg DIC/yr. Both of these freshwater displacement effects are nontrivial compared to the estimated 58 ± 10 Tg/yr carbon air-sea uptake: $\tilde{T}_C^{PER}$ drives much of the observed transport of DIC (see Text S3, Table S1 in Supporting Information S1).

This regrouping allows direct comparison of the budget terms between the inversion and state estimate (Figures 2b–2e). Quantitative agreement is imprecise due to differing time periods, inexact alignment of boundaries (see Figure 1a), and ambiguities inherent in extrapolating summertime measurements to a multi-annual average. $\tilde{T}_C^{PER}$ is weaker in the inversion, though more similar to the B-SOSE summertime value (−64 ± 8 Tg DIC/yr) than to the annual average (−75 ± 5 Tg DIC/yr). Inversion-derived $\tilde{T}_C^{SI}$ is stronger than the minimal B-SOSE summer value but far weaker than the annual average, since sea-ice export occurs during winter. Interestingly, $-\hat{T}_C$ is negative (−19 ± 11 Tg DIC/yr) in the inversion but positive year-round in B-SOSE; this is likely related to the strong horizontal net outward transport of DIC found in the inverse solution (MacGilchrist et al., 2019). The inversion uses a multidecadal trend in interior ocean DIC concentration to reflect an annual mean; its 5 ± 1 Tg/yr DIC is considerably weaker than B-SOSE's estimate and other observational estimates (see Text S2, Figure S5 in Supporting Information S1). Finally, the inversion assumes that biological processes have no mean effect on DIC, whereas in B-SOSE they drive both an annual cycle and a significant mean loss of DIC.

4. Conclusions and Implications

We have shown that the displacement of seawater by net precipitation and glacial melt $\left(\tilde{T}_C^{PER}\right)$ and by sea ice export $\left(\tilde{T}_C^{SI}\right)$ constitute leading order terms in the full Weddell Gyre carbon budget, both in our B-SOSE experiments and in a new decomposition of ANDREX inverse model transports (Brown et al., 2015; Jullion et al., 2014; MacGilchrist et al., 2019). These freshwater displacement effects are separate from the dilution of surface waters by sea ice melt, which strongly influences DIC concentrations (Hoppema et al., 1999; Rosso et al., 2017) but which does not generate any DIC mass transport. The B-SOSE estimate during the 2013–2021 period shows that $\tilde{T}_C^{PER}$ plays the central role in removing carbon from the Weddell Gyre at a rate of 75 ± 5 Tg DIC per year, driven primarily by year-round net precipitation. This is partially compensated by the import of seawater in response to the export of sea ice, which draws a transport of $\tilde{T}_C^{SI} = -48 \pm 11$ Tg/yr DIC southward into the region; during this under-observed winter season, B-SOSE shows that displacement effects dominate the carbon budget. We also computed the strength of the displacement effects in published inverse estimates of the carbon transport into the Weddell Gyre, and found that $\tilde{T}_C^{SI} = -12 \pm 2$ Tg/yr and especially $\tilde{T}_C^{PER} = 44 \pm 5$ Tg/yr are key components of the total 51 ± 10 Tg/yr DIC transport out of the gyre. Thus freshwater processes are central to not only carbon concentrations but also net carbon transport in the Weddell Gyre via freshwater displacement effects.

Given the challenges in observing and modeling the Weddell Gyre and the significant discrepancies between our estimates, we should consider how realistic the magnitudes of $\tilde{T}_C^{PER}$ and $\tilde{T}_C^{SI}$ are likely to be. Our estimates of the displacement effects are simply the product of two quantities: the relevant volume transport $\tilde{T}_V$ and the DIC concentration difference between the freshwater and displaced seawater. The volume transports of net precipitation, glacial melt, and sea ice export are modified through complex inverse calculations from prior values (i.e., initial guesses), which are in turn derived from reanalysis and satellite data products (except for B-SOSE's sea ice transport, which is dynamically derived). B-SOSE and the inverse model from Jullion et al. (2014) use similar priors, but B-SOSE strengthens each transport and the inverse model weakens them, as shown in Table S2 in Supporting Information S1. The summertime observational bias is likely a driver of these consistent differences, especially for disparate estimates of sea ice transport (see Text S4 in Supporting Information S1). As for the carbon concentration difference, our estimate is slightly too high: We have assumed 0 freshwater DIC concentration, which is reasonable for meteoric water (with 1% the DIC concentration of seawater) but less so for sea ice, which has mean DIC concentrations of 0.27 ± 0.10 mmol/kg (12 ± 5% of seawater) (Fransson et al., 2011). Our seawater concentration estimates are well constrained, thanks to the relatively uniform oceanic DIC concentration

19448007, 2023, 18, Downloaded from https://agupubs.onlinelibrary.wiley.com/doi/10.1029/2023GL103952 by University Of California, Wiley Online Library on [20/02/2024]. See the Terms and Conditions (https://onlinelibrary.wiley.com/terms-and-conditions) on Wiley Online Library for rules of use; OA articles are governed by the applicable Creative Commons License

across the Weddell Gyre boundary (see Figure S1 in Supporting Information S1). In summary, $\tilde{T}_C^{PER}$ is fairly well constrained, whereas $\tilde{T}_C^{SI}$ is more poorly constrained from observations and systematically overrepresented by B-SOSE's lack of sea ice DIC; still, both terms should be considered significant components of carbon transport.

With a clear example of the freshwater displacement effect on carbon transport in the Weddell Gyre, we consider whether this effect could have a similarly prominent role in the full Southern Ocean. While we lack hydrographic estimates of carbon transport on this scale, we can readily compute the total meridional carbon transport and freshwater displacement effect in B-SOSE (Figure 3). Very far south, $\tilde{T}_C^{PER}$ and $\tilde{T}_C^{SI}$ nearly compensate each other, with $\tilde{T}_C^{SI}$ leading around 70°S (Figure 3a). However, southward oceanic transport proportional to northward sea ice advection is confined to the sea ice zone (south of 55°S). In contrast, net precipitation drives a strong northward transport throughout the Southern Ocean; this is the oceanic return of the southward transport of moisture by mid-latitude storms (Wijffels et al., 1992). $\tilde{T}_C^{PER}$ imprints strongly on the total carbon transport across the mid-latitude Southern Ocean (Figure 3b). Indeed, when B-SOSE was run with freshwater fluxes represented by virtual salt fluxes (see Methods) such that the freshwater displacement effect was not active, the net meridional carbon transport is in the opposite direction (Figure 3b). This remaining net southward transport of DIC (brown) is essentially $\hat{T}_C$, which is due to the higher DIC concentrations in the southward limb of the overturning compared with the northward limb. When the freshwater displacement effect $\left(\tilde{T}_C\right)$ is computed separately and added, the result compares well with our "real freshwater" run, although there are other differences between the runs. These full-basin calculations affirm that the freshwater displacement effect can be understood as the imprint of the global water cycle - moisture transport in the atmosphere and cryosphere reciprocated by ocean volume transport - on oceanic carbon transport. This imprint is striking because the DIC concentration difference between seawater and meteoric water is much larger than the concentration differences between oceanic watermasses; the steady northward displacement of DIC meaningfully opposes the net southward transport by the overturning circulation in the Weddell Gyre and beyond.

The significance of freshwater displacement to observed oceanic carbon transport has been identified by a few previous studies (Holfort et al., 1998; Robbins, 2001; Stoll et al., 1996) but overlooked by several others (Álvarez et al., 2003; Brewer et al., 1989; Broecker & Peng, 1992; Brown et al., 2015; MacGilchrist et al., 2019); no study has considered the displacement effect of sea ice transport, especially its significant seasonal cycle. These relatively small divergent volume transports cannot be resolved by box inverse solutions for velocity, implying that carbon transports calculated directly from inverse model velocities will include large errors in $\tilde{T}_C$ (Robbins, 2001). However, within a closed domain, $\tilde{T}_C$ can be precisely calculated by computing the total freshwater divergence utilizing the conservation of salt (Schauer & Losch, 2019; Wijffels et al., 1992). This relationship can be employed toward a salinity-normalized carbon transport (Broecker & Peng, 1992) which avoids calculating the freshwater displacement effect; however, salinity normalization is only valid if salt is perfectly balanced, and moreover it ignores the key processes transporting carbon (Robbins, 2001). In the Weddell Gyre, Jullion et al. (2014) included a model-derived eddy transport that balances the mean geostrophic volume transport and the diagnosed freshwater transport, somewhat obscuring the relevance of freshwater input to the net outflow (see Text S3 in Supporting Information S1). MacGilchrist et al. (2019) includes the carbon carried by this net outflow in the overturning term of the overturning-horizontal decomposition (Bryden & Imawaki, 2001); their small overturning transport results from the compensation of the overturning DIC import and the freshwater displacement effect, as occurs widely across the Southern Ocean in B-SOSE (Figure 3b). We encourage explicit calculation of the freshwater displacement effect on carbon transport via the net freshwater divergence in future work.

This is to our knowledge the first modeling study to highlight freshwater displacement effects on oceanic carbon transport, particularly its dependence on representation of freshwater fluxes. Ocean models were historically unable to simulate freshwater displacement effects because of their virtual tracer fluxes, which represent only the dilution effect of freshwater input (Griffies et al., 2001) (see Methods). Replacing a virtual tracer flux with a real freshwater flux makes an immediate, first-order impact on the Southern Ocean meridional carbon transport (Figure 3b). Furthermore, with "real freshwater" turned on, net transport of DIC is closely related to the cumulative air-sea uptake in the multi-annual average, as predicted from a box model perspective (though differences, e.g., at 40°S, are present due to changes in the oceanic storage of DIC). In the virtual tracer flux run, this relationship is absent due to non-conservation of DIC mass: net precipitation results in a net removal of DIC from the surface ocean via the virtual flux, rather than a realistic displacement of oceanic DIC northward. Thus, use of "real freshwater" fluxes seems imperative for comparisons with observed carbon transport; however, studies performing an inversion of interior ocean carbon observations via model-derived ocean transports have

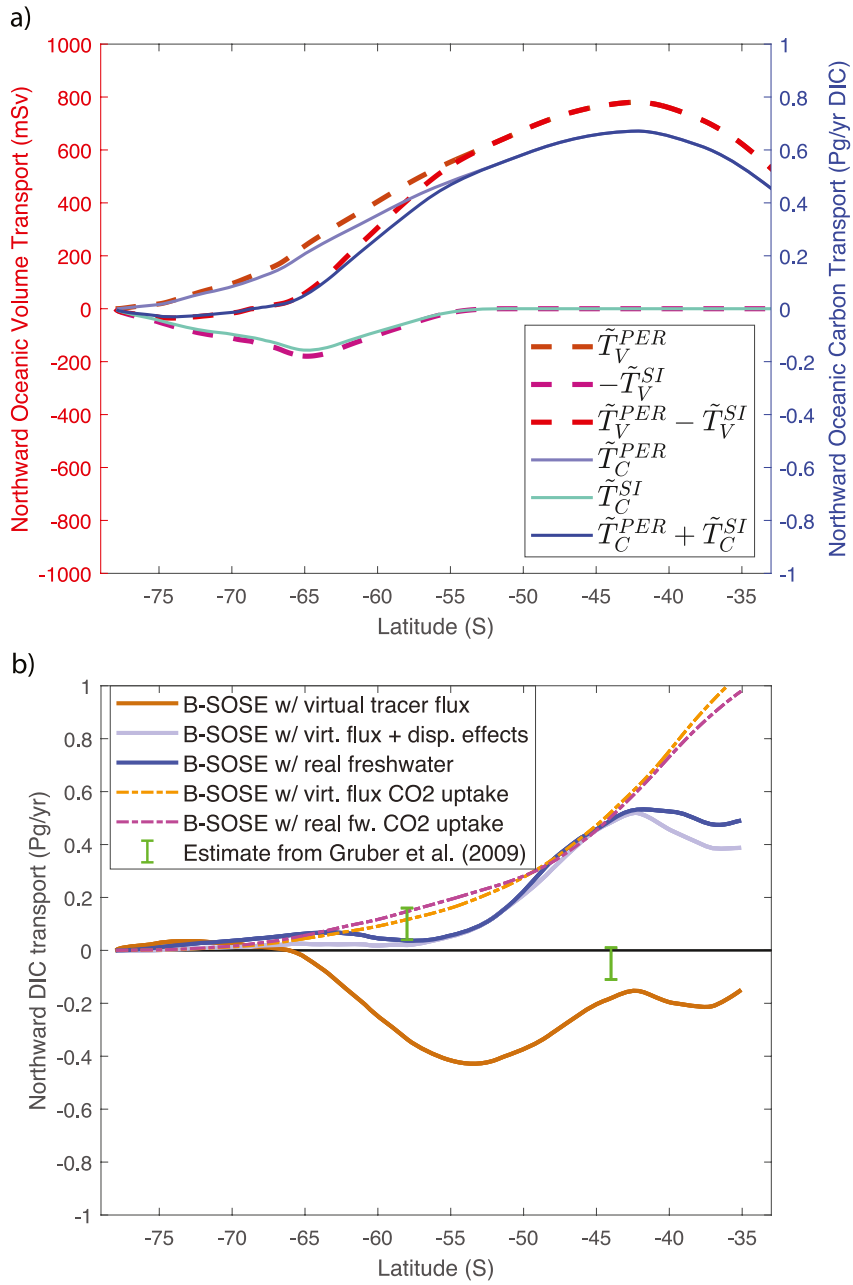

Figure 3. Zonally Averaged Freshwater Displacement Effect on Meridional Transport of dissolved inorganic carbon (DIC) in B-SOSE. (a) Dashed lines show B-SOSE Iteration 139 2013–2021 mean meridional volume transport for the full Southern Ocean, decomposed into transports driven by net P-E+R (integrated south of the given latitude) and sea ice transport (northward sea ice transport $\tilde{T}_V^{SI}$ drives ocean water southward). Solid lines show B-SOSE Iteration 139 2013–2021 mean freshwater displacement effects on meridional carbon transport, with the circumpolar average evaluated at each latitude. These differ from the volume transports by a factor of the zonally and vertically averaged DIC concentration, which varies only slightly through the global ocean. (b) We compare the zonally integrated northward DIC transport over the 2013–2017 period between "B-SOSE w/virtual tracer flux" (Iteration 122, with no freshwater displacement) and "B-SOSE w/real freshwater flux" (Iteration 139, with freshwater displacement). Plotted second is the sum of the "B-SOSE w/virtual tracer flux" total transport and the diagnosed $\tilde{T}_C$ in Iteration 139 (2013–2017 mean). Also shown is the Southern Ocean air-sea flux of CO_2 in B-SOSE, here integrated southward to Antarctica from each latitude, for both runs. Finally, estimates of meridional DIC transport at 58°S and 44°S during 1995–2000 Gruber et al. (2009) are plotted for reference.

19448007, 2023, 18, Downloaded from https://agupubs.onlinelibrary.wiley.com/doi/10.1029/2023GL103952 by University Of California, Wiley Online Library on [20/02/2024]. See the Terms and Conditions (https://onlinelibrary.wiley.com/terms-and-conditions) on Wiley Online Library for rules of use; OA articles are governed by the applicable Creative Commons License

19448007, 2023, 18, Downloaded from https://agupubs.onlinelibrary.wiley.com/doi/10.1029/2023GL103952 by University Of California, Wiley Online Library on [20/02/2024]. See the Terms and Conditions (https://onlinelibrary.wiley.com/terms-and-conditions) on Wiley Online Library for rules of use; OA articles are governed by the applicable Creative Commons License

frequently compared them with ocean models with virtual fluxes (Gloor et al., 2003; Gnanadesikan et al., 2004; Jacobson et al., 2007a; Mikaloff Fletcher et al., 2007). While the details of the methods (e.g., the salinity normalization scheme) employed therein are beyond our scope, the virtual flux may have led to misrepresentation of the freshwater displacement effect; indeed, internal inconsistencies between transport and surface flux estimates were largest in the mid-latitude Southern Ocean, where the freshwater transport is strongest (Gloor et al., 2003; Gruber et al., 2009; Jacobson et al., 2007b). Given the relative magnitude of the freshwater displacement effect for DIC, we recommend against the use of virtual tracer fluxes for studies of carbon (Yin et al., 2010) - even in models focused on processes affecting DIC concentration in the surface ocean (Rosso et al., 2017).

While the consequences of freshwater displacement effects may be wide-reaching, we emphasize that our understanding arises from focused regional comparison of model and hydrographic datasets. Box inverse estimates provided a benchmark pointing to inconsistencies (namely, the virtual flux) in our model representation; analysis of the corrected model clarified drivers of observed transport, particularly the role of freshwater displacement in the surprisingly small overturning-driven DIC transport in MacGilchrist et al. (2019). B-SOSE analysis can be of great utility to ongoing hydrographic campaigns, informing assumptions around extending quasi-synoptic summer observations (e.g., of DIC advection) to annual means and estimating terms beyond our present observational capability (e.g., net effect of biology on DIC); in order to apply these results to observations, clear understanding of discrepancies between observed and modeled DIC concentration trends and $\hat{T}_C$ would be required (see Text S1, Figure S4 in Supporting Information S1).

Changing Antarctic freshwater fluxes are linked to carbon-climate feedbacks via their potential to alter the partitioning of carbon between atmosphere and deep ocean (Nissen et al., 2022; Stephens & Keeling, 2000). As our ability to observe and model the seasonal sea ice zone advances, their synergy should help us pinpoint how the processes shaping modern-day gas exchange there contribute to past and future climate change. The freshwater displacement effect described here provides a direct connection between changing ice-ocean-atmosphere freshwater fluxes and oceanic carbon transport; changes in transport must be compensated by other terms in the carbon budget. Predicted increases in precipitation and particularly meltwater (Pattyn & Morlighem, 2020) would displace oceanic carbon northward, opposing the increased upwelling (net southward) transport of DIC driven by strengthening westerly winds (Bronselaer et al., 2020). These same winds may also increase sea ice export (Haumann et al., 2016), leading to a freshwater displacement effect driving carbon toward Antarctica; however, the consequences of recent decreases in Antarctic sea ice extent remain unknown. While freshwater displacement alone encourages oceanic sequestration of carbon, simultaneous responses to freshwater input (e.g., strengthened halocline, increased biological production) must also be considered; analysis of perturbation experiments together with ongoing biogeochemical observations should investigate the interplay of changing lateral carbon transports with the stratifying upper ocean.

Data Availability Statement

This study used the B-SOSE model output iteration 139 and iteration 122, which is available at http://sose.ucsd.edu/SO6/ITER139 and http://sose.ucsd.edu/SO6/ITER122 (Verdy & Mazloff, 2022). This data processed with Matlab (R2020b) and Jupyter Notebook, with code stored at https://doi.org/10.5281/zenodo.8088294. The hydrographic data used in Figure S1 in Supporting Information S1 is freely available at the CCHDO website (https://cchdo.ucsd.edu/cruise/74JC20100319, https://cchdo.ucsd.edu/cruise/740H20081226, and https://cchdo.ucsd.edu/cruise/33RR20080204). Grateful acknowledgment to the captains and crews of these ships and the data analysis and storage communities involved. The ERA5 reanalysis is available at https://www.ecmwf.int/en/forecasts/datasets/reanalysis-datasets/era5.

Acknowledgments
This work was funded by NSF's Southern Ocean Carbon and Climate Observations and Modeling (SOCCOM) Project under NSF awards PLR-1425989 and OPP-1936222. G.A.M was additionally supported under UKRI Grant MR/W013835/1. M.R.M. also acknowledges support from NASA grant 80NSSC20K1076 and NSF grants OCE-1924388 and OPP-2149501. Thanks to Jorge Sarmiento, F. Alex Haumann, Stephen Griffies, and Tyler Rohr for their helpful comments. Col. 2:3, Psalm 65:5.

References

Abernathey, R. P., Cerovecki, I., Holland, P. R., Newsom, E., Mazloff, M., & Talley, L. D. (2016). Water-mass transformation by sea ice in the upper branch of the Southern Ocean overturning. *Nature Geoscience*, *9*(8), 596–601. https://doi.org/10.1038/ngeo2749

Álvarez, M., Ríos, A. F., Pérez, F. F., Bryden, H. L., & Rosón, G. (2003). Transports and budgets of total inorganic carbon in the subpolar and temperate North Atlantic. *Global Biogeochemical Cycles*, *17*(1), 2–1. https://doi.org/10.1029/2002GB001881

Brewer, P. G., Goyet, C., & Dyrssen, D. (1989). Carbon dioxide transport by ocean currents at 25N latitude in the Atlantic Ocean. *Science*, *246*(4929), 477–479. https://doi.org/10.1126/science.246.4929.477

Broecker, W. S., & Peng, T.-H. (1992). Interhemispheric transport of carbon dioxide by ocean circulation. *Nature*, *356*(6370), 587–589. https://doi.org/10.1038/356587a0

Bronselaer, B., Russell, J. L., Winton, M., Williams, N. L., Key, R. M., Dunne, J. P., et al. (2020). Importance of wind and meltwater for observed chemical and physical changes in the Southern Ocean. *Nature Geoscience*, *13*(1), 35–42. https://doi.org/10.1038/s41561-019-0502-8

Brown, P. J., Jullion, L., Landschützer, P., Bakker, D. C. E., Naveira Garabato, A. C., Meredith, M. P., et al. (2015). Carbon dynamics of the Weddell Gyre, Southern Ocean. *Global Biogeochemical Cycles*, *29*(3), 288–306. https://doi.org/10.1002/2014GB005006

Bryden, H. L., & Imawaki, S. (2001). Ocean heat transport. *International Geophysics*, *77*, 455–474.

Campin, J.-M., Adcroft, A., Hill, C., & Marshall, J. (2004). Conservation of properties in a free-surface model. *Ocean Modelling*, *6*(3–4), 221–244. https://doi.org/10.1016/S1463-5003(03)00009-X

Delille, B., Vancoppenolle, M., Geilfus, N.-X., Tilbrook, B., Lannuzel, D., Schoemann, V., et al. (2014). Southern Ocean CO_2 sink: The contribution of the sea ice. *Journal of Geophysical Research: Oceans*, *119*(9), 6340–6355. https://doi.org/10.1002/2014JC009941

Fransson, A., Chierici, M., Yager, P. L., & Smith, W. O., Jr. (2011). Antarctic sea ice carbon dioxide system and controls. *Journal of Geophysical Research*, *116*(C12), C12035. https://doi.org/10.1029/2010JC006844

Gloor, M., Gruber, N., Sarmiento, J., Sabine, C. L., Feely, R. A., & Rödenbeck, C. (2003). A first estimate of present and preindustrial air-sea CO_2 flux patterns based on ocean interior carbon measurements and models. *Geophysical Research Letters*, *30*(1), 10-1–10-4. https://doi.org/10.1029/2002GL015594

Gnanadesikan, A., Dunne, J. P., Key, R. M., Matsumoto, K., Sarmiento, J. L., Slater, R. D., & Swathi, P. (2004). Oceanic ventilation and biogeochemical cycling: Understanding the physical mechanisms that produce realistic distributions of tracers and productivity. *Global Biogeochemical Cycles*, *18*(4), GB4010. https://doi.org/10.1029/2003GB002097

Gray, A. R., Johnson, K. S., Bushinsky, S. M., Riser, S. C., Russell, J. L., Talley, L. D., et al. (2018). Autonomous biogeochemical floats detect significant carbon dioxide outgassing in the high-latitude southern ocean. *Geophysical Research Letters*, *45*(17), 9049–9057. https://doi.org/10.1029/2018GL078013

Griffies, S. M., Pacanowski, R. C., Schmidt, M., & Balaji, V. (2001). Tracer conservation with an explicit free surface method for z-coordinate ocean models. *Monthly Weather Review*, *129*(5), 1081–1098. https://doi.org/10.1175/1520-0493(2001)129<1081:tcwaef>2.0.co;2

Gruber, N., Gloor, M., Mikaloff Fletcher, S. E., Doney, S. C., Dutkiewicz, S., Follows, M. J., et al. (2009). Oceanic sources, sinks, and transport of atmospheric CO_2. *Global Biogeochemical Cycles*, *23*(1), GB1005. https://doi.org/10.1029/2008GB003349

Hall, M. M., & Bryden, H. L. (1982). Direct estimates and mechanisms of ocean heat transport. *Deep Sea Research Part A. Oceanographic Research Papers*, *29*(3), 339–359. https://doi.org/10.1016/0198-0149(82)90099-1

Haumann, F. A., Gruber, N., Münnich, M., Frenger, I., & Kern, S. (2016). Sea-ice transport driving Southern Ocean salinity and its recent trends. *Nature*, *537*(7618), 89–92. https://doi.org/10.1038/nature19101

Holfort, J., Johnson, K., Schneider, B., Siedler, G., & Wallace, D. W. (1998). Meridional transport of dissolved inorganic carbon in the South Atlantic Ocean. *Global Biogeochemical Cycles*, *12*(3), 479–499. https://doi.org/10.1029/98GB01533

Hoppema, M., Fahrbach, E., Stoll, M. H., & de Baar, H. J. (1999). Annual uptake of atmospheric CO_2 by the Weddell Sea derived from a surface layer balance, including estimations of entrainment and new production. *Journal of Marine Systems*, *19*(4), 219–233. https://doi.org/10.1016/s0924-7963(98)00091-8

Hoppema, M., Roether, W., Bellerby, R. G., & de Baar, H. J. (2001). Direct measurements reveal insignificant storage of anthropogenic CO_2 in the abyssal Weddell Sea. *Geophysical Research Letters*, *28*(9), 1747–1750. https://doi.org/10.1029/2000gl012443

Huang, R., & Schmitt, R. (1993). The Goldsbrough–Stommel circulation of the world oceans. *Journal of Physical Oceanography*, *23*(6), 1277–1284. https://doi.org/10.1175/1520-0485(1993)023<1277:tgcotw>2.0.co;2

Iudicone, D., Rodgers, K. B., Stendardo, I., Aumont, O., Madec, G., Bopp, L., et al. (2011). Water masses as a unifying framework for understanding the Southern Ocean Carbon Cycle. *Biogeosciences*, *8*(5), 1031–1052. https://doi.org/10.5194/bg-8-1031-2011

Jacobson, A. R., Mikaloff Fletcher, S. E., Gruber, N., Sarmiento, J. L., & Gloor, M. (2007a). A joint atmosphere-ocean inversion for surface fluxes of carbon dioxide: 1. Methods and global-scale fluxes. *Global Biogeochemical Cycles*, *21*(1), GB1020. https://doi.org/10.1029/2006GB002703

Jacobson, A. R., Mikaloff Fletcher, S. E., Gruber, N., Sarmiento, J. L., & Gloor, M. (2007b). A joint atmosphere-ocean inversion for surface fluxes of carbon dioxide: 2. Regional results. *Global Biogeochemical Cycles*, *21*(1), GB1019. https://doi.org/10.1029/2005GB002556

Jullion, L., Garabato, A. C. N., Bacon, S., Meredith, M. P., Brown, P. J., Torres-Valdés, S., et al. (2014). The contribution of the Weddell Gyre to the lower limb of the Global Overturning Circulation. *Journal of Geophysical Research: Oceans*, *119*(6), 3357–3377. https://doi.org/10.1002/2013JC009725

MacGilchrist, G. A., Garabato, A. C. N., Brown, P. J., Jullion, L., Bacon, S., Bakker, D. C., et al. (2019). Reframing the carbon cycle of the subpolar Southern Ocean. *Science Advances*, *5*(8), eaav6410. https://doi.org/10.1126/sciadv.aav6410

Mikaloff Fletcher, S., Gruber, N., Jacobson, A. R., Gloor, M., Doney, S., Dutkiewicz, S., et al. (2007). Inverse estimates of the oceanic sources and sinks of natural CO_2 and the implied oceanic carbon transport. *Global Biogeochemical Cycles*, *21*(1), GB1010. https://doi.org/10.1029/2006GB002751

Murnane, R., Sarmiento, J. L., & Le Quéré, C. (1999). Spatial distribution of air-sea co2 fluxes and the interhemispheric transport of carbon by the oceans. *Global Biogeochemical Cycles*, *13*(2), 287–305. https://doi.org/10.1029/1998GB900009

Nicholls, K. W., Østerhus, S., Makinson, K., Gammelsrød, T., & Fahrbach, E. (2009). Ice-ocean processes over the continental shelf of the southern Weddell Sea, Antarctica: A review. *Reviews of Geophysics*, *47*(3), RG3003. https://doi.org/10.1029/2007RG000250

Nissen, C., Timmermann, R., Hoppema, M., Gürses, Ö., & Hauck, J. (2022). Abruptly attenuated carbon sequestration with Weddell Sea dense waters by 2100. *Nature Communications*, *13*(1), 3402. https://doi.org/10.1038/s41467-022-30671-3

Pattyn, F., & Morlighem, M. (2020). The uncertain future of the Antarctic Ice Sheet. *Science*, *367*(6484), 1331–1335. https://doi.org/10.1126/science.aaz5487

Pellichero, V., Sallée, J.-B., Chapman, C. C., & Downes, S. M. (2018). The Southern Ocean meridional overturning in the sea-ice sector is driven by freshwater fluxes. *Nature Communications*, *9*(1), 1–9. https://doi.org/10.1038/s41467-018-04101-2

Robbins, P. E. (2001). Oceanic carbon transport carried by freshwater divergence: Are salinity normalizations useful? *Journal of Geophysical Research*, *106*(C12), 30939–30946. https://doi.org/10.1029/2000JC000451

Roemmich, D., & Wunsch, C. (1985). Two transatlantic sections: Meridional circulation and heat flux in the subtropical North Atlantic Ocean. *Deep Sea Research Part A. Oceanographic Research Papers*, *32*(6), 619–664. https://doi.org/10.1016/0198-0149(85)90070-6

Rosso, I., Mazloff, M. R., Verdy, A., & Talley, L. D. (2017). Space and time variability of the Southern Ocean carbon budget. *Journal of Geophysical Research: Oceans*, *122*(9), 7407–7432. https://doi.org/10.1002/2016JC012646

Sarmiento, J. L., Murnane, R., & Le Quere, C. (1995). Air—sea CO_2 transfer and the carbon budget of the north Atlantic. *Philosophical Transactions of the Royal Society of London. Series B: Biological Sciences*, *348*(1324), 211–219. https://doi.org/10.1098/rstb.1995.0063

Sarmiento, J. L., & Toggweiler, J. (1984). A new model for the role of the oceans in determining atmospheric pCO_2. *Nature*, *308*(5960), 621–624. https://doi.org/10.1038/308621a0

19448007, 2023, 18, Downloaded from https://agupubs.onlinelibrary.wiley.com/doi/10.1029/2023GL103952 by University Of California, Wiley Online Library on [20/02/2024]. See the Terms and Conditions (https://onlinelibrary.wiley.com/terms-and-conditions) on Wiley Online Library for rules of use; OA articles are governed by the applicable Creative Commons License

Schauer, U., & Losch, M. (2019). "Freshwater" in the ocean is not a useful parameter in climate research. *Journal of Physical Oceanography*, *49*(9), 2309–2321. https://doi.org/10.1175/JPO-D-19-0102.1

Sigman, D. M., Hain, M. P., & Haug, G. H. (2010). The polar ocean and glacial cycles in atmospheric CO_2 concentration. *Nature*, *466*(7302), 47–55. https://doi.org/10.1038/nature09149

Stephens, B. B., & Keeling, R. F. (2000). The influence of Antarctic sea ice on glacial–interglacial CO_2 variations. *Nature*, *404*(6774), 171–174. https://doi.org/10.1038/35004556

Stoll, M., Van Aken, H., De Baar, H., & De Boer, C. (1996). Meridional carbon dioxide transport in the northern North Atlantic. *Marine Chemistry*, *55*(3–4), 205–216. https://doi.org/10.1016/S0304-4203(96)00057-6

Talley, L. D., Rosso, I., Kamenkovich, I., Mazloff, M. R., Wang, J., Boss, E., et al. (2019). Southern Ocean biogeochemical float deployment strategy, with example from the Greenwich Meridian line (GO-SHIP A12). *Journal of Geophysical Research: Oceans*, *124*(1), 403–431. https://doi.org/10.1029/2018JC014059

Thompson, L., Smith, M., Thomson, J., Stammerjohn, S., Ackley, S., & Loose, B. (2020). Frazil ice growth and production during katabatic wind events in the Ross Sea, Antarctica. *The Cryosphere*, *14*(10), 3329–3347. https://doi.org/10.5194/tc-14-3329-2020

Tréguier, A.-M., Deshayes, J., Le Sommer, J., Lique, C., Madec, G., Penduff, T., et al. (2014). Meridional transport of salt in the global ocean from an eddy-resolving model. *Ocean Science*, *10*(2), 243–255. https://doi.org/10.5194/os-10-243-2014

Verdy, A., & Mazloff, M. (2022). Biogeochemical Southern Ocean State Estimate, iteration 139 [Dataset]. UCSD Library. Retrieved from http://sose.ucsd.edu/SO6/ITER139/

Verdy, A., & Mazloff, M. R. (2017). A data assimilating model for estimating Southern Ocean biogeochemistry. *Journal of Geophysical Research: Oceans*, *122*(9), 6968–6988. https://doi.org/10.1002/2016JC012650

Vernet, M., Geibert, W., Hoppema, M., Brown, P. J., Haas, C., Hellmer, H., et al. (2019). The Weddell Gyre, Southern Ocean: Present knowledge and future challenges. *Reviews of Geophysics*, *57*(3), 623–708. https://doi.org/10.1029/2018RG000604

Wijffels, S. E., Schmitt, R. W., Bryden, H. L., & Stigebrandt, A. (1992). Transport of freshwater by the oceans. *Journal of Physical Oceanography*, *22*(2), 155–162. https://doi.org/10.1175/1520-0485(1992)022<0155:tofbto>2.0.co;2

Yin, J., Stouffer, R. J., Spelman, M. J., & Griffies, S. M. (2010). Evaluating the uncertainty induced by the virtual salt flux assumption in climate simulations and future projections. *Journal of Climate*, *23*(1), 80–96. https://doi.org/10.1175/2009JCLI3084.1

References From the Supporting Information

Galbraith, E. D., Gnanadesikan, A., Dunne, J. P., & Hiscock, M. R. (2010). Regional impacts of iron-light colimitation in a global biogeochemical model. *Biogeosciences*, *7*(3), 1043–1064. https://doi.org/10.5194/bg-7-1043-2010

Gruber, N., Clement, D., Carter, B. R., Feely, R. A., Van Heuven, S., Hoppema, M., et al. (2019). The oceanic sink for anthropogenic CO_2 from 1994 to 2007. *Science*, *363*(6432), 1193–1199. https://doi.org/10.1126/science.aau5153

Hammond, M. D., & Jones, D. C. (2016). Freshwater flux from ice sheet melting and iceberg calving in the Southern Ocean. *Geoscience Data Journal*, *3*(2), 60–62. https://doi.org/10.1002/gdj3.43

Harms, S., Fahrbach, E., & Strass, V. H. (2001). Sea ice transports in the Weddell Sea. *Journal of Geophysical Research*, *106*(C5), 9057–9073. https://doi.org/10.1029/1999JC000027

Mazloff, M. R., Heimbach, P., & Wunsch, C. (2010). An eddy-permitting Southern Ocean state estimate. *Journal of Physical Oceanography*, *40*(5), 880–899. https://doi.org/10.1175/2009JPO4236.1

Nicolas, J. P., & Bromwich, D. H. (2011). Precipitation changes in high southern latitudes from global reanalyses: A cautionary tale. *Surveys in Geophysics*, *32*(4), 475–494. https://doi.org/10.1007/s10712-011-9114-6

Nie, Y., Uotila, P., Cheng, B., Massonnet, F., Kimura, N., Cipollone, A., & Lv, X. (2022). Southern Ocean sea ice concentration budgets of five ocean-sea ice reanalyses. *Climate Dynamics*, *59*(11–12), 1–21. https://doi.org/10.1007/s00382-022-06260-x

Talley, L. D. (2008). Freshwater transport estimates and the global overturning circulation: Shallow, deep and throughflow components. *Progress in Oceanography*, *78*(4), 257–303. https://doi.org/10.1016/j.pocean.2008.05.001

van Heuven, S. M., Hoppema, M., Huhn, O., Slagter, H. A., & de Baar, H. J. (2011). Direct observation of increasing CO_2 in the Weddell Gyre along the Prime Meridian during 1973–2008. *Deep Sea Research Part II: Topical Studies in Oceanography*, *58*(25–26), 2613–2635. https://doi.org/10.1016/j.dsr2.2011.08.007

19448007, 2023, 18, Downloaded from https://agupubs.onlinelibrary.wiley.com/doi/10.1029/2023GL103952 by University Of California, Wiley Online Library on [20/02/2024]. See the Terms and Conditions (https://onlinelibrary.wiley.com/terms-and-conditions) on Wiley Online Library for rules of use; OA articles are governed by the applicable Creative Commons License